



2017

Multi-Band Antenna Array Based on Double Negative Metamaterial for Multi Automotive Applications

Mohd Jamlos

Universiti Malaysia Perlis

Abdulrahman Alqadami,

Universiti Malaysia Perlis

Imtiaz Islam

Universiti Malaysia Perlis

Ping Soh


Universiti Malaysia Perlis

Rizalman Mamat

Universiti Malaysia Pahang, Pekan 26600, Malaysia.

See next page for additional authors

Follow this and additional works at: <http://arrow.dit.ie/ahfrcart>

 Part of the [Computer Engineering Commons](#), and the [Systems and Communications Commons](#)

Recommended Citation

Alqadami, A. et al. et al. (2017) Multi-Band Antenna Array Based on Double Negative Metamaterial for Multi Automotive Applications, *PROGRESS IN ELECTROMAGNETICS RESEARCH-PIER*, 159 27-37; 2017, Unique ID: WOS:000411498900003

This Article is brought to you for free and open access by the Antenna & High Frequency Research Centre at ARROW@DIT. It has been accepted for inclusion in Articles by an authorized administrator of ARROW@DIT. For more information, please contact yvonne.desmond@dit.ie, arrow.admin@dit.ie, brian.widdis@dit.ie.



This work is licensed under a [Creative Commons Attribution-NonCommercial-Share Alike 3.0 License](#)



Authors

Mohd Jamlos; Abdulrahman Alqadami,; Imtiaz Islam; Ping Soh; Rizalman Mamat; Khairil Khairi; and Adam Narbudowicz

Multi-Band Antenna Array Based on Double Negative Metamaterial for Multi Automotive Applications

Abdulrahman S. M. Alqadami¹, Mohd F. Jamlos^{1, 2, *}, Imtiaz Islam¹, Ping J. Soh¹, Rizalman Mamat², Khairil A. Khairi^{1, 3}, and Adam Narbudowicz^{4, 5}

Abstract—This paper presents a design of multi-band array antenna based on Double Negative Metamaterial (DNM) unit cells for multi-automotive applications. The antenna consists of 4×4 rectangular and circular radiating patches connected in series using microstrip lines and fed by a 50Ω corporate microstrip line. An array of 4×6 wire loaded complementary spiral resonator (CSR) unit cells is placed on its reverse side to provide miniaturization and multiband features to the proposed design. The reflection coefficient (S_{11}), mutual coupling, effective diversity gain (EDG), envelope correlation coefficient (ECC), and radiation patterns are evaluated for four elements of the proposed antenna placed in four different locations on the car body model. Simulations and measurements indicated that the proposed antenna features a low mutual coupling (< -34 dB), low ECC (< 0.01), high EDG (> 9.995), high efficiency (72%–95%), and low on-car detuning over the desired five bands; 1.99 GHz to 3.03 GHz, 5.15 GHz to 6.369 GHz, 7.67 GHz to 7.99 GHz, 9.91 GHz to 10.23 GHz, and 11.79 GHz to 12.2 GHz. The performance of ECC between four antennas on car body has been investigated in different cases of isotropic, indoor, and outdoor. The metallic effect on antennas performance also has been investigated by evaluating the mutual coupling and transmission coefficient between two antennas served as transmitter and receiver with presence of car body. The results show transmission coefficient of proposed DNM antenna with metallic presence almost identical to free space across desired frequency bands. With all capabilities mentioned the antenna has potential for WiFi/WiMAX, Vehicle-to-Vehicle (V2V), transportable earth exploration satellite, military requirement for land vehicles, and earth stations on vessels applications.

1. INTRODUCTION

Nowadays, the demand for antennas in wireless communication system for automotive applications is rising at a rapid rate [1, 2]. Their usage includes collision avoidance system (CAS), Vehicle-to-vehicle communications, pre-crash safety systems, Global Positioning Systems (GPS), tyre pressure monitoring system (TPMS), Wireless Local Area Network (WLAN), etc. To enhance its effectiveness in these new applications, a small, multi-band, multi-functional antenna is required instead of conventional single band antennas [2, 3]. Such multifunctional antennas with favourable radiation characteristics are more practical in addressing modern antenna design requirements. However, the achievement of the above mentioned antenna's features using conventional materials and structures is challenging [4].

One popular solution to improve the electromagnetic waves characteristics and physical features of antennas is to use metamaterial unit cells structures [5]. Metamaterials are materials typically

Received 12 September 2016, Accepted 18 April 2017, Scheduled 10 June 2017

* Corresponding author: Mohd Faizal Jamlos (mohdfaizaljamlos@gmail.com).

¹ Advanced Communication Engineering Centre (ACE), School of Computer & Communication Engineering, Universiti Malaysia Perlis, Malaysia. ² Faculty of Mechanical Engineering, Universiti Malaysia Pahang, Pekan 26600, Malaysia. ³ Jabil Circuit, Plot 56, Bayan Lepas Industrial Park, Phase 4, Penang 11900, Malaysia. ⁴ Dublin Institute of Technology, Kevin Street, Dublin 8, Ireland. ⁵ Institute of High Frequency Technology, RWTH Aachen University, Melatener Str. 25, Aachen 52074, Germany.

engineered using synthetic structures to produce exceptional electromagnetic properties that could not be achieved in nature [6]. In particular, metamaterials with negative permittivity and permeability are now used in antenna designs that exhibit a high size miniaturization factor with multiband behaviour [7]. Double negative material was first implemented in a periodic array using split ring resonators and wire strips [6]. The excitation of number of split ring resonators (SRRs) and long wire strips enabled a structure that has both negative magnetic properties (from the SRRs) and negative dielectric features (from the wire strips). Their electromagnetic wave characteristics are retrieved by studying the transmission and reflection parameters [8]. Rather than using split ring resonators and wire strips, a wire loaded CSR can exhibit characteristics of a DNM with increased miniaturization factor and multiple operating frequency bands for an antenna [9].

In this research, we propose a 4×4 series-fed antenna array loaded with a 4×6 CSR DNM array of unit cells. The proposed antenna sized at $0.24\lambda \times 0.4\lambda \times 0.004\lambda$ operates in five frequency bands centered at 2.4, 5.9, 7.8, 10 and 12 GHz. The antenna is assessed on a car's body in four locations; front, back, right and left. To our best knowledge, this is the first antenna based on DNM investigated for automotive applications. It provides a low mutual coupling, low ECC, high EDG, and radiation efficiency of at least 72% within its operating bands. Moreover, the transmission coefficient of the proposed antenna for assessing the car body metal influence on antenna performance are analyzed as well. Its omnidirectional radiation characteristics are also validated to be suited for multi-functional vehicular applications. The next section describes the antenna topology and the CSR unit cells, followed by the investigation of its performance in free space and when placed on a car at different locations in Section 3. Finally, we conclude this work in Section 4.

2. ANTENNA DESIGN AND FABRICATION PROCEDURE

2.1. Design of the Wire Loaded CSR Unit Cell

The proposed CSR uses a Rogers RT/Duroid 5880 substrate with a permittivity (ϵ_r) of 2.2, loss tangent ($\tan\delta$) of 0.0009 and thickness of 0.51 mm. It consists of three wire rings, and each smaller ring is connected to the outer ring with 0.45 mm width. Its geometrical parameters are tabulated in Table 1.

Table 1. Dimensions of the antenna and CSR cells.

Parameter	Value (mm)	Parameter	Value (mm)	Parameter	Value (mm)
w_p	5.25	$w_6 \& w_7$	0.6	g_u	0.55
l_p	5.25	w_8	0.8	m	1.55
a	5	l_1	1	g	0.55
w_1	0.6	l_2	3	w_{sr1}	6
w_2	1	l_3	14.6	w_{sr2}	3.9
$w_3 \& w_4$	0.6	l_g	5	w_{sr3}	1.8
w_5	0.8	l_u	4.2	g_s	0.6

In this work, the unit cell is simulated using finite-difference time domain (FDTD) solver in CST Microwave Studio to obtain S -parameters (S_{11} , and S_{21}). Figure 1(a) demonstrates the simulation setup for the proposed unit cell. It has been positioned between two identical waveguide ports on the positive and negative z -axis with a 50Ω impedance. The reflection coefficient (S_{11}) and transmission coefficient (S_{21}) then obtained by the instantaneous excitation of magnetic and electrical dipoles incident on the proposed CSR unit cell and plotted in Figure 1(c). The effective permittivity, permeability and refractive index retrieved from S_{11} and S_{21} using common method known as S -parameters retrieval that has been introduced in [8]. The effective metamaterial parameters then extracted using equations as described in [8, 9]:

$$z = \sqrt{\frac{(1 + S_{11})^2 - S_{21}^2}{(1 - S_{11})^2 - S_{21}^2}} \quad (1)$$

$$e^{(jnk_0d)} = X \pm j\sqrt{1 - X^2} \tag{2}$$

$$X = \frac{(1 - S_{11}^2 + S_{21}^2)}{2S_{21}} \tag{3}$$

$$n = \frac{1}{k_0 \cdot d} \text{Cos}^{-1} \left(\frac{1}{2S_{21}} (1 - S_{11}^2 + S_{21}^2) \right) \tag{4}$$

$$\varepsilon = \frac{n}{z}, \quad \text{and} \quad \mu = n \times Z \tag{5}$$

where k_0 , d , Z , n , ε , and μ are the wave vector of the incident wave, thickness of the unit cell slab, impedance, refractive index, the relative effective permittivity, and the relative effective permeability, respectively. The effective permittivity, permeability and refractive index are illustrated in Figures 1(d) and (e).

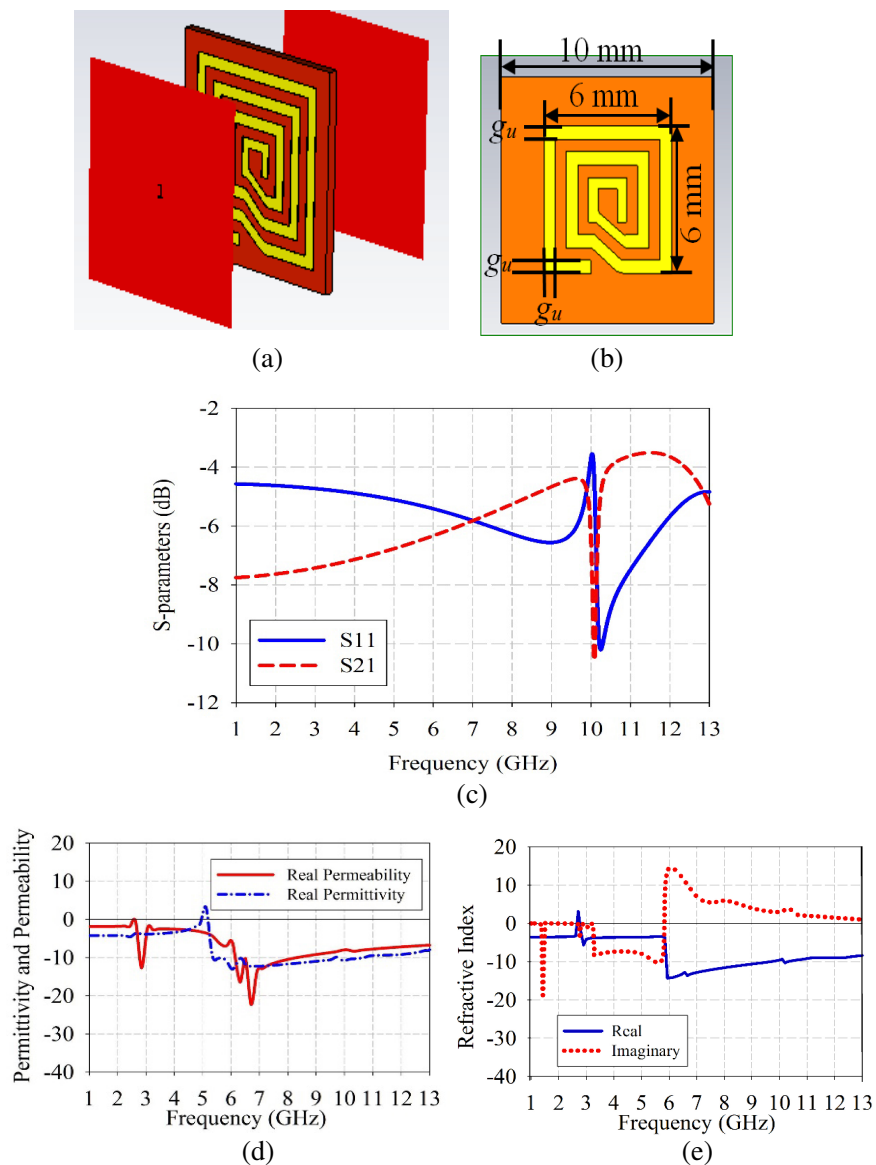


Figure 1. (a) CSR unit cell setup in CST, (b) dimensions of the CSR unit cell, (c) S -parameters of unit cell, (d) real μ_{eff} and ε_{eff} , (e) extracted real refractive index.

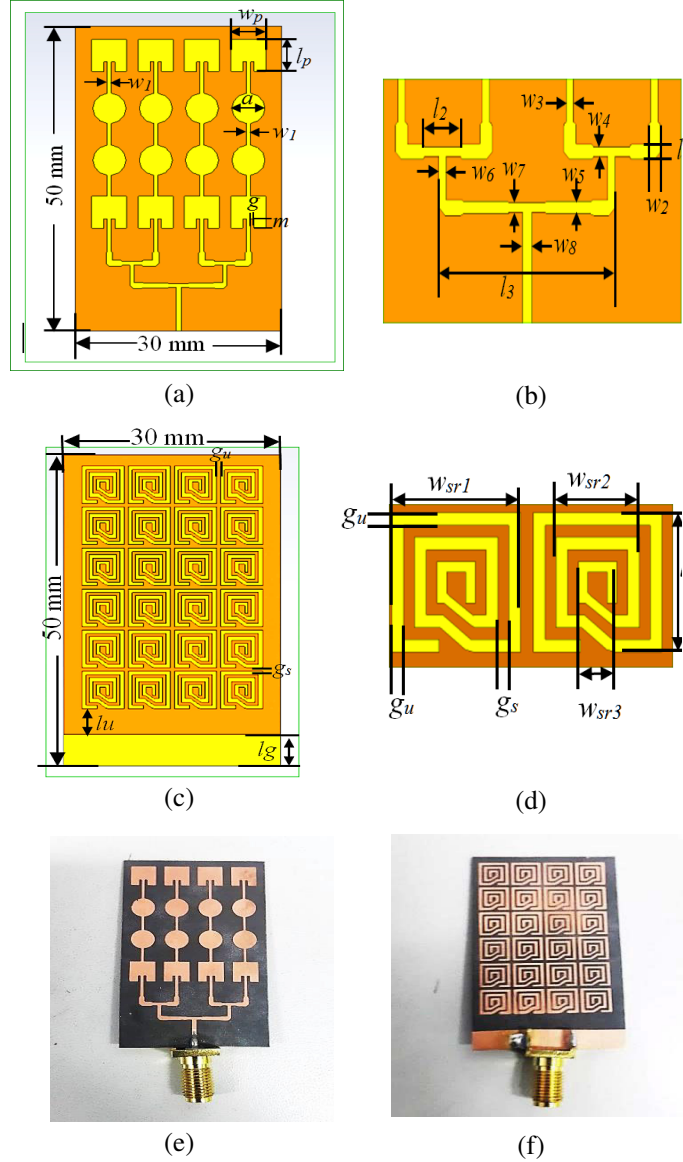


Figure 2. The geometry and dimensions of the proposed antenna: (a) front view, (b) corporate feed network, (c) CSR structure, (d) unit cell, (e) fabricated prototype front view, and (f) rear view.

2.2. Antenna Design

Figure 2 illustrates the topology of the proposed antenna array. A microstrip array is chosen in this work due to its planar structure and ease of integration with other microwave structures in automobile applications [10]. The array is formed on a RT/Duroid 5880 substrate using 16-rectangular and circular radiating elements and is fed by a combination of series and corporate feed network as shown in Figures 2(a) and (b). Meanwhile, an array of 24 CSR unit cells is placed on the reverse side of the antenna, in proximity of a partial ground plane, see Figures 2(c) and (d). Figures 2(e) and (f) illustrate the fabricated prototype of the proposed antenna.

3. EXPERIMENTAL RESULTS AND DISCUSSION

The proposed antenna is first assessed in free space prior to its performance evaluation on a car model. Figure 3 depicts the reflection coefficient, gain and efficiency. Reflection coefficients (S_{11}) are below -16 dB within the operating frequency bands. The optimum antenna gain of 7.5 dB is achieved in the

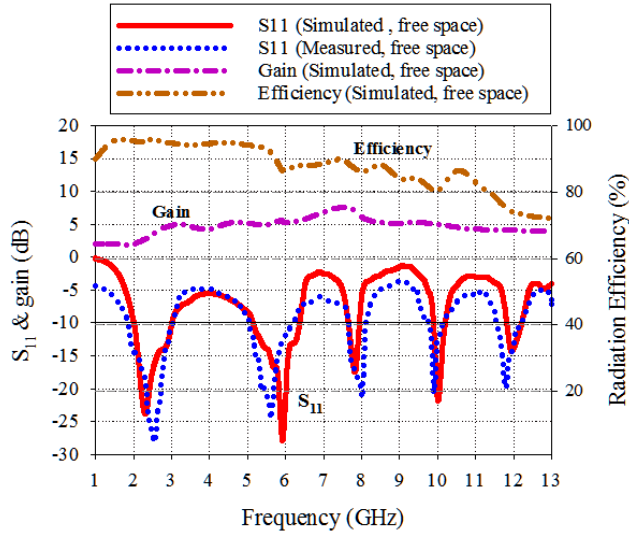


Figure 3. Simulated and measured results of the proposed antenna in free space, simulated and measured S_{11} , gain and efficiency of the proposed antenna with integration of metamaterial unit cells.

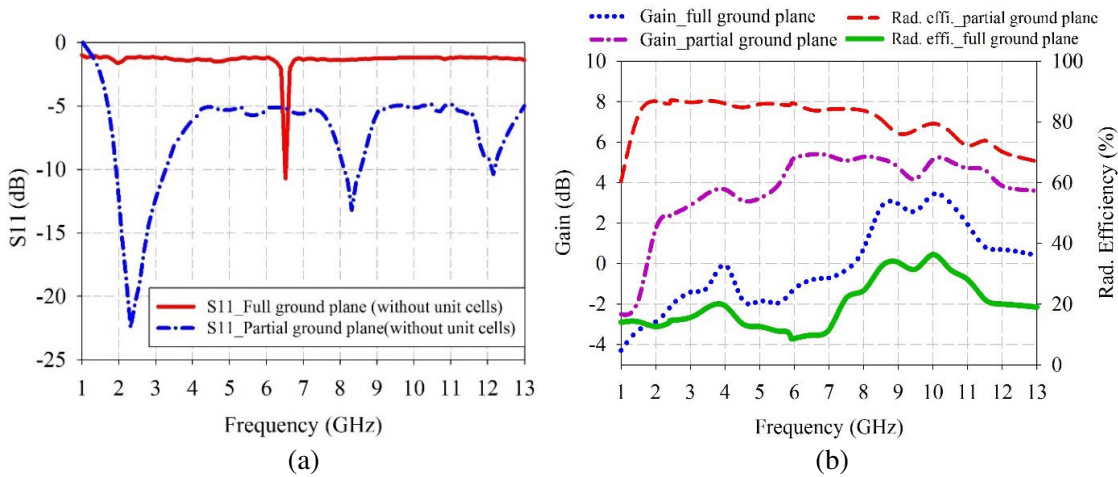


Figure 4. Simulated results of the proposed antenna in free space without metamaterial unit cells, (a) simulated S_{11} of the proposed antenna without metamaterial unit cells, (b) simulated gain and efficiency of the proposed antenna without metamaterial unit cells.

third band. Nonetheless, gain of the antenna remained between 3 dB and 5 dB in the other bands. In general, the radiation efficiency of the proposed antenna is satisfactory in all bands as can be seen in Figure 3. Higher radiation efficiencies, with a maximum of 95% is observed in the lower bands due to decreased losses.

Additionally, the performance of the proposed antenna array (S_{11} , gain and efficiency) is evaluated by simulation when the metamaterial unit cells are not presented. The first evaluation was performed when the antenna is partially grounded ($l_g = 5$ mm). The result of S_{11} is presented in Figure 4(a). The second and the fourth bands were eliminated. Moreover, the gain and efficiency of the antenna are slightly decreased (see Figure 4(b)) in comparison with metamaterial antenna. The second investigation was performed when the antenna has no unit cells and fully grounded with copper. The antenna observed to operate only at a single band of 6.5 GHz while the remaining bands are eliminated as can be seen in Figure 4(a). Furthermore, the gain and efficiency of the antenna are significantly dropped as depicted by Figure 4(b).

This section describes the antenna performance by placing it on a car body. The car used in this work is Opel Tuned model shown in Figure 5 where the rear quarter window and antennas are

clearly seen. The model has been derived from CAD data, refined and cleaned into a suitable with detail electromagnetic model as depicted in Figure 5. The model combines both external and internal components as inner door skins, steering mechanism and internal furnished things. Those parts have been omitted in the simulation in order to keep it as simple as possible. CST microwave studio has been used for simulation based on finite integration time domain method. The CAD model has been inserted as “Object” file, and the direct importation of this “obj” into the simulation tool faces difficulties. This is due to the size of the car model which is very large compared to antenna and overall mesh provided by the simulator was very high. Furthermore, it needs simplification to reduce the car body size with mesh which has been solved using “mm” scale. After simplification. It is sized at 3.4 m (length) by 1.6 m (width), resulting in a total mesh of about 200 million. The simulation has been proceeded using high performance work station. Four antennas were installed at four locations; front (Antenna 1), rear (Antenna 2), right (Antenna 3) and left (Antenna 4) as depicted by Figures 5(a) and (b). Those four antennas have been placed in four different locations for acquiring better coverage. Both bumper positions were chosen (antenna 1 and antenna 2) to evaluate antennas performance with other communication system like sensors. In order to investigate the technical parameter performance of the antennas with the sides of car body, antenna 3 and 4 have been chosen as it is observed that

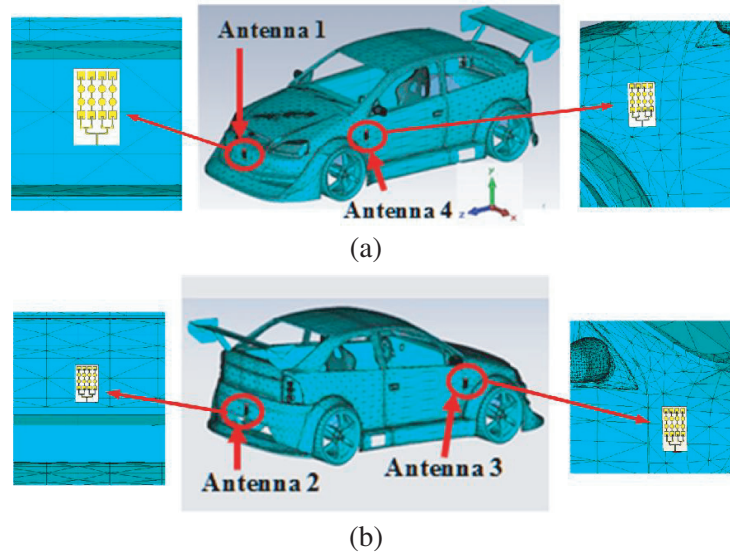


Figure 5. Car model setup, (a) front and left side view, (b) back and right side view.

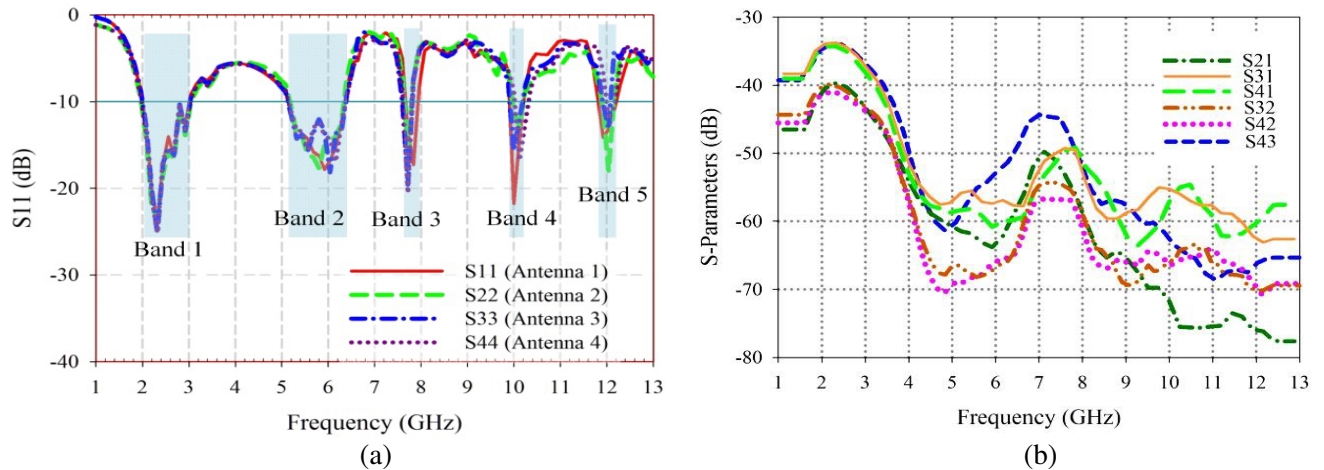


Figure 6. Reflection coefficient (S_{11}) and mutual coupling of four antennas on car body model, (a) S_{11} , (b) mutual coupling.

the behaviour of those antennas is quiet good. Antennas 1&2 and antennas 3&4 have been placed at same alignment and in the flat portion of car body so that it can be fully attached with car body. Such location is important to evaluate radiations and mutual coupling between antennas that can be used for multiplicity applications.

Figures 6(a) and (b) illustrate the simulated reflection coefficients ($S_{11}, S_{22}, S_{33}, S_{44}$) and mutual coupling ($S_{21}, S_{31}, S_{41}, S_{23}, S_{24}, S_{34}$) between all four antennas. The reflection coefficients for all antennas placed on the car is below -15 dB while mutual coupling stated of more than 34 dB in all bands. It is observed that mutual coupling is affected by the distance, positions and medium including metallic car body, see Figure 6(b). It shows that position of the antenna is effected more compared to frequency which dictate a uniform pattern. For example, at the frequency of 7.67 GHz, the S_{43} (antenna's position of left and right) shows the higher mutual coupling effect compared to $S_{21}, S_{31}, S_{41}, S_{32}$ and S_{42} . Nonetheless, S_{43} still scores a good coupling value of -45 dB. This proves that the coupling of S_{43} which is separated by three layers, two metals and a hollow in between has minimum impact on mutual coupling. Such low mutual coupling indicates that the metallic car body has slightly effect on reflection coefficients and mutual coupling of the antennas at different positions and subsequently improve the channel capacity of the multi antennas across the five desired bands.

Instead of mutual coupling, more comprehensive investigation on the metallic body effect on antenna performance is realized by analyzing the insertion loss (S_{21}). Here, the S_{21} is a parameter of transmission coefficient and not the mutual coupling. Figure 7(a) shows the free space simulation setup while 7(b) simulates two antennas separated by a metallic body with 7.69×10^6 S/m electrical conductivity. Note that antenna 1 serves as a transmitter and antenna 2 serves as a receiver.

Figure 7(c) shows S_{21} of between -35 dB and -62 dB when both antennas are radiated in free space. However, it is noted that the transmission coefficient of metallic car body presence is almost identical with free space. In theory, objects in contact or in close proximity to an antenna, such as high-loss and high-dielectric human body and metallic objects, will severely degrade the antenna radiation

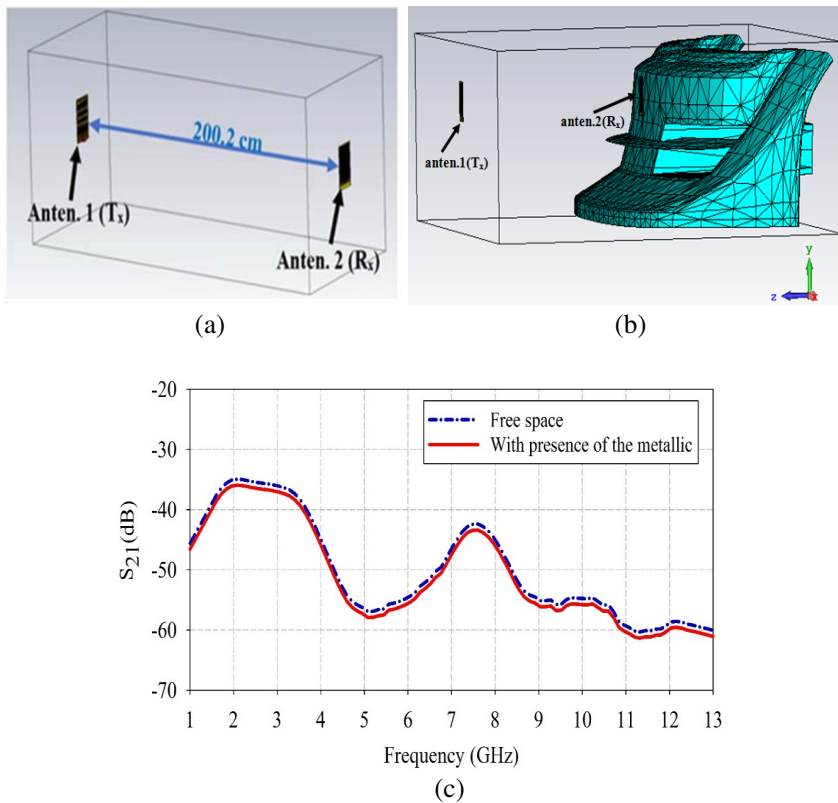


Figure 7. Effect of metallic car body on transmission coefficient, (a) free space setup, (b) with presence of metallic car body, (c) transmission coefficient, S_{21} .

efficiency due to reduction in the antenna radiation resistance [11].

By intuition, the antenna tends to radiate efficiently when the antenna electrical size is in the same range as the wavelength, indicating that favourable antenna geometry is required for good radiation efficiency performance as well. Thus, for a minimum frequency of 1.99 GHz, the electrical length of the antenna should more than $15.789 \times 15.789 \text{ cm}^2$. However, the proposed DNG metamaterial antenna designed with dimension of $5.0 \times 3.0 \text{ cm}^2$ managed to have a very minimum transmission degradation. Nonetheless, such minimum degradation caused by the metallic body still be acceptable. This is due to a small loss resistance that is in the same order of magnitude as the radiation resistance, which is enough to sustain the radiation efficiency, contributed by the proposed DNG metamaterial antenna.

On the other hand, two critical parameters to characterize the multi-antenna capability are the envelope correlation coefficient (ECC) and effective diversity gain (EDG). Diversity performance between antennas can be evaluated by envelop correlation coefficient (ECC) which can be determined

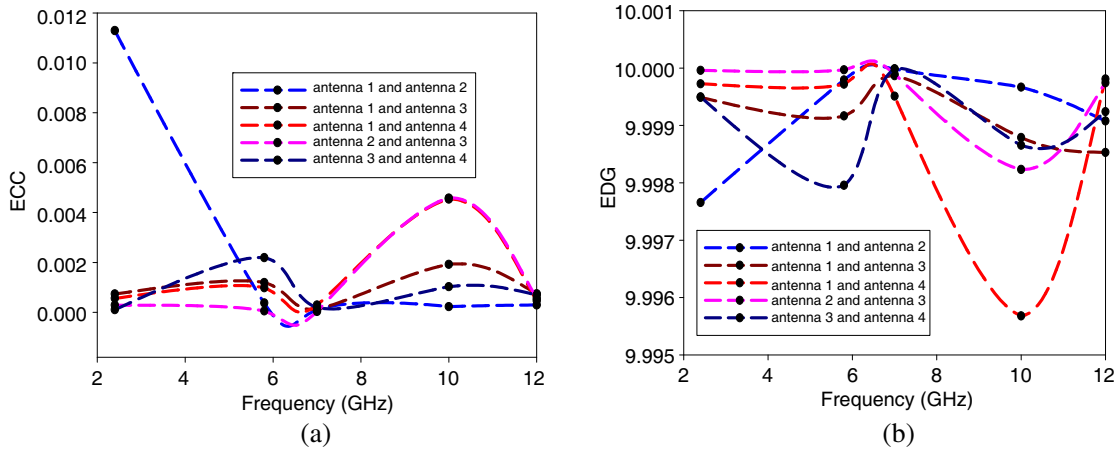


Figure 8. (a) Envelope correlation coefficient (ECC) on outdoor ($XPR = 1$), (b) effective diversity gain (EDG) between all antennas placed on the car model.

Table 2. ECC on different cases at different frequencies.

ECC	Antenna	2.4 GHz	5.8 GHz	7 GHz	10 GHz	12 GHz
Isotropic ($XPR = 0 \text{ dB}$)	Antenna 1&2	0.0010787346	9.5290221e-005	8.1525599e-006	0.00015365961	0.00042494841
	Antenna 1&3	0.00012626794	0.00013070887	0.00022614272	0.001987678	8.8625779e-005
	Antenna 1&4	0.00023650575	0.0003844915	6.1780274e-005	0.00055821852	0.00067712465
	Antenna 2&3	0.00085543158	0.00016962968	0.00016464585	0.0011105556	0.00019953483
	Antenna 3&4	0.00023138241	0.00094116897	7.5042356e-006	0.00061989582	0.00035041429
Indoor ($XPR = 6 \text{ dB}$)	Antenna 1&2	0.0010787346	9.5290221e-005	8.1525599e-006	0.00015365961	0.00042494841
	Antenna 1&3	0.0007740999	0.0028278659	0.000265233	0.0071682005	5.5511179e-005
	Antenna 1&4	0.00090254202	0.001974702	0.00051551326	0.0042447797	0.00049824204
	Antenna 2&3	0.00035578317	7.9123808e-005	2.9178901e-005	0.0041363787	4.6553634e-005
	Antenna 3&4	0.00085051138	0.0077975108	0.00027681544	0.0014243462	0.0030566522

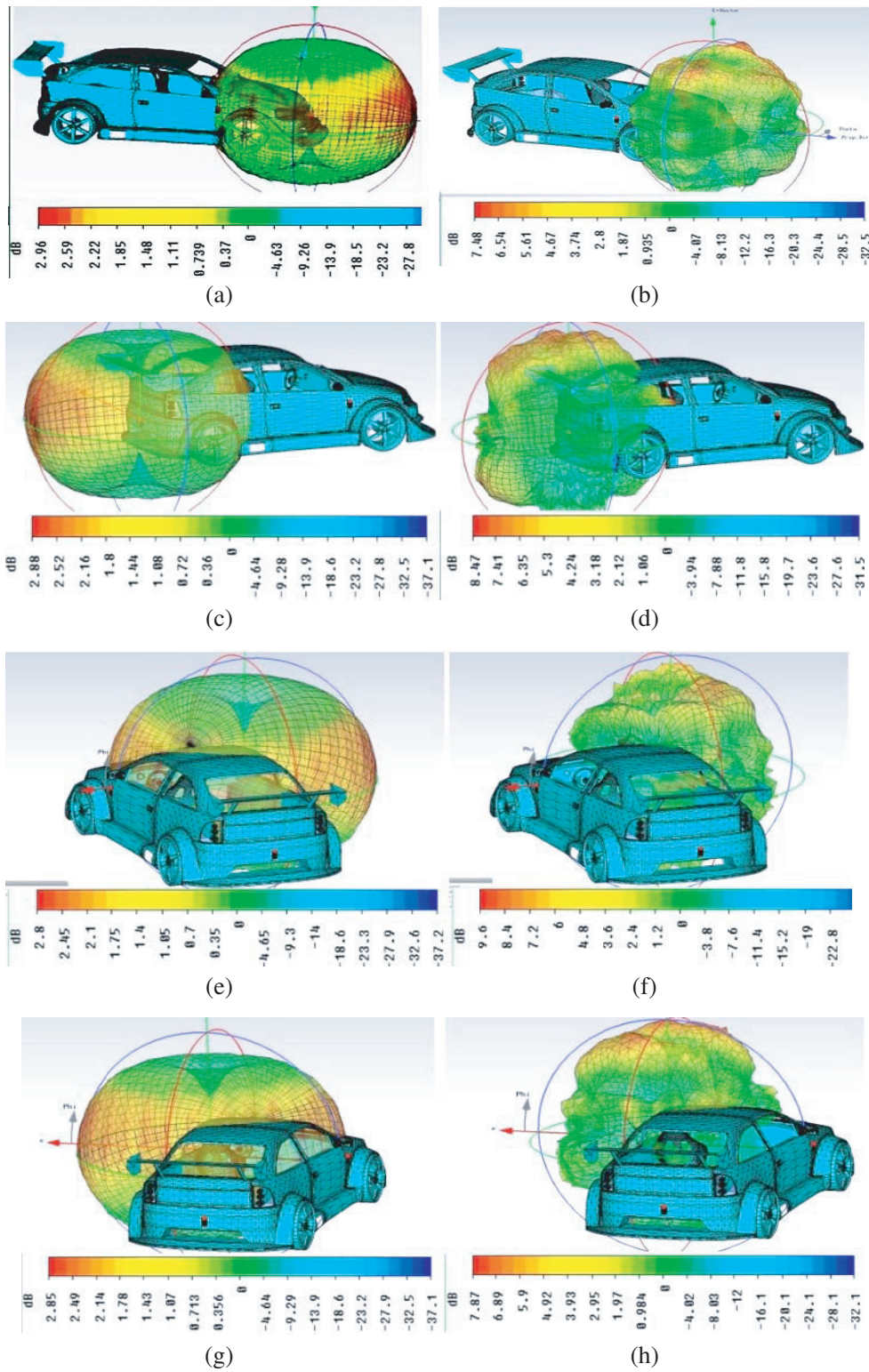


Figure 9. Three-dimensional radiation patterns of the proposed antenna placed on the car model. (a) at 2.4 GHz (for Antenna 1), (b) at 12 GHz (for Antenna 1), (c) at 2.4 GHz (for Antenna 2), (d) at 12 GHz (for Antenna 2), (e) at 2.4 GHz (for Antenna 3), (f) at 12 GHz (for Antenna 3), (g) at 2.4 GHz (for Antenna 4), (h) at 12 GHz (for Antenna 4).

from total far field radiation pattern [12]. The effectiveness of diversity in term of diversity gain can be calculated using Eq. (6) [13]

$$\text{EDG} = 10 * \sqrt{(1 - |\text{Ecc}|)} \quad (6)$$

Figure 8 demonstrates variation of ECC and EDG of the four antennas on the car model. For evaluating envelop correlation coefficient between four antennas on car body, different cases have been considered. Figure 8(a) depicts the ECC on outdoor cases where cross polarization ratio (XPR) = 1 is implemented using Gaussian for elevation and uniform for azimuth [12]. It shows that a low ECC (< 0.01) have been achieved in all cases when the four antennas are placed on car body while Figure 8(b) depicts that EDG which are computed at 1% are closely to 10dB across desired bands. Such results proven that the antennas applied on the car model have a good diversity performance and suitable channel characteristics. This is further strengthened by Table 2 which presents the other two cases of ECC which are isotropic where XPR = 0 and indoor cases where XPR = 6.

Figure 9 depicts the 3D radiation patterns of the four antennas on car body model. For the sake of brevity, three-dimensional radiation patterns are presented for two bands: at 2.4 GHz (first band) and 12 GHz (fifth band). As can be observed form Figures 10(a)–(h), the gain of the antennas have been increased (up to 9 dB at 12 GHz) when they are placed on car body due to the present of metallic surface. It acts as a reflector for the antennas and the radiation patterns become slightly directed toward the free space [14].

Figure 10 presents the simulated and measured radiation patterns of the proposed antenna in

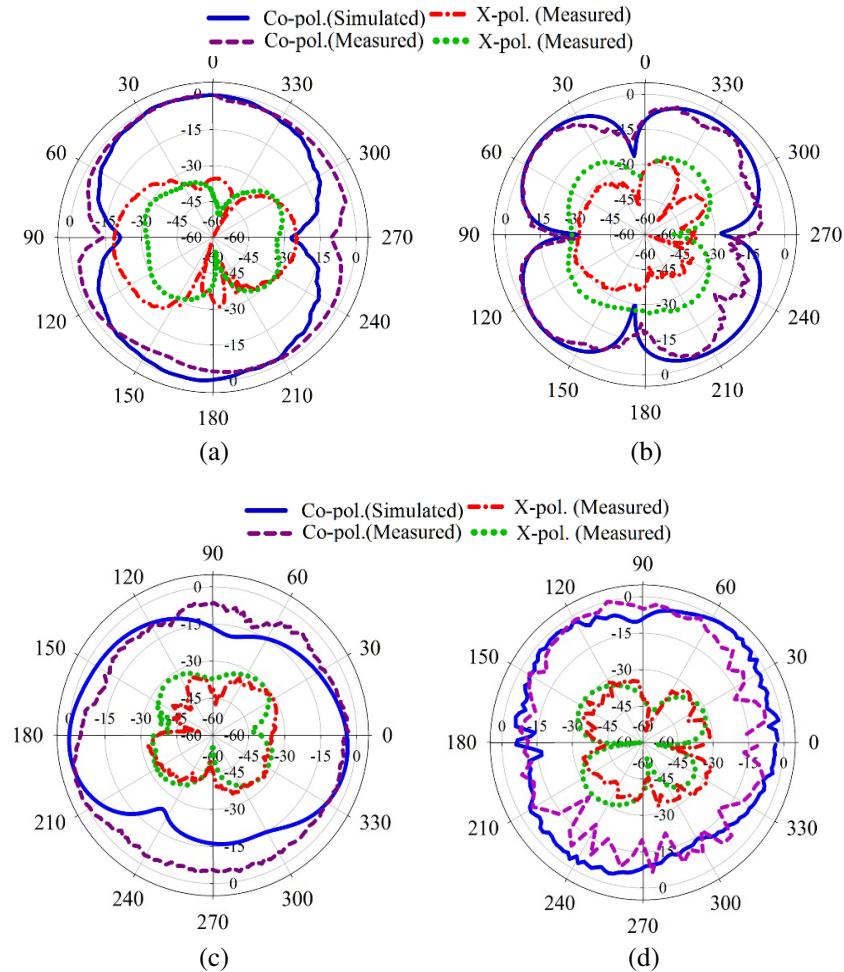


Figure 10. Radiation patterns of the proposed antenna (in the H -plane), (a) 2.4 GHz, (b) 5.9 GHz, (c) 7.8 GHz, (d) 10 GHz.

the H -plane at 2.4 GHz, 5.9 GHz, 7.8 GHz, and 10 GHz. Measurements were performed in an anechoic chamber using a E8051C Network Analyzer. The measured radiation patterns agree well with simulation indicating that the proposed antenna has good performance.

4. CONCLUSION

A multi-band array based on Double Negative Metamaterial (DNM) unit cells for vehicular applications is presented. The proposed antenna covers five bands with center frequencies at 2.4/5.9/7.8/10/12 GHz which can fulfill the requirement of WiFi/WiMAX, vehicle to vehicle (V2V), transportable earth exploration satellite, military requirement for land vehicles, and earth stations on vessels applications, respectively. Its performance is first evaluated in free space. It is then placed on four different locations of a car model, excited simultaneously and examined in terms of reflection coefficient, antennas mutual coupling, ECC, EDG, insertion loss and radiation patterns. The proposed antenna shows an excellent capability of mitigating detuning caused by the body of the car by featuring a low mutual coupling (< -34 dB), low ECC (< 0.01), high EDG (> 9.99) and good radiations features.

REFERENCES

1. Bilgic, M. M. and K. Yegin, "Modified annular ring antenna for GPS and SDARS automotive applications," *IEEE Antennas Wireless Propag. Lett.*, Vol. 15, 1442–1445, 2016.
2. Mondal, T., S. Samanta, R. Ghatak, and S. R. Bhadra Chaudhuri, "A novel tri-band hexagonal microstrip patch antenna using modified sierpinski fractal for vehicular communication," *Progress In Electromagnetics Research C*, Vol. 57, 25–34, 2015.
3. Zhou, Y., C.-C. Chen, and J. L. Volakis, "Dual band proximity-fed stacked patch antenna for tri-band GPS applications," *IEEE Trans. Antennas Propag.*, Vol. 55, No. 1, 220–223, 2007.
4. Rafaei Booket, M., A. Jafargholi, M. Kamyab, H. Eskandari, M. Veysi, and S. M. Mousavi, "Compact multi-band printed dipole antenna loaded with single-cell metamaterial," *IET Micro., Antennas & Prop.*, Vol. 6, No. 1, 17–23, 2012.
5. Sato, K., S. H. Yonak, T. Nomura, S. I. Matsuzawa, and H. Iizuka, "Metamaterials for automotive applications," *IEEE Antenn. Propag. Soc. Inter. Symp.*, 1144–1147, Honolulu, HI, 2007.
6. Smith, D. R., W. J. Padilla, D. C. Vier, S. C. Nemat-Nasser, and S. Schultz, "Composite medium with simultaneously negative permeability and permittivity," *Phys. Rev. Lett.*, Vol. 84, No. 18, 4184–4187, 2000.
7. Xie, Y. H., C. Zhu, L. Li, and C. H. Liang, "A novel dual-band metamaterial antenna based on complementary split ring resonators," *Microw. Opt. Technol. Lett.*, Vol. 54, 1007–1009, 2012.
8. Smith, D. R. and S. Schultz, "Determination of effective permittivity and permeability of metamaterials from reflection and transmission coefficients," *Phys. Rev. B*, Vol. 65, 195104, 2002.
9. Smith, D., D. Vier, T. Koschny, and C. Soukoulis, "Electromagnetic parameter retrieval from inhomogeneous metamaterials," *Phys. Rev. E*, Vol. 71, 036617, 2005.
10. Rabinovich, V. and N. Alexandrov, *Antenna Arrays and Automotive Applications*, Springer-Verlag, New York, 2013.
11. Koski, E., T. Björninen, L. Ukkonen, and L. Sydänheimo, "Radiation efficiency measurement method for passive UHF RFID dipole tag antennas," *IEEE Trans. Antennas Propag.*, Vol. 61, No. 8, 4026–4035, 2013.
12. Singh, H. S., B. R. Meruva, G. K. Pandey, P. K. Bharti, and M. K. Meshram, "Low mutual coupling between MIMO antennas by using two folded shorting strips," *Progress In Electromagnetics Research B*, Vol. 53, 205–221, 2013.
13. Schwartz, M., W. R. Bennett, and S. Stein, *Communication System and Techniques*, 470–474, McGraw-Hill, New York, NY, USA, 1965.
14. Kim, J. K., I. Y. Oh, T. W. Koo, J. C. Kim, D. S. Kim, and J. G. Yook, "Effects of a metal plane on a meandered slot antenna for UHF RFID applications," *Journal of Electromagnetic Engineering and Science*, Vol. 12, No. 2, 176–184, 2012.